

## Eta Photoproduction

Lothar Tiator\* and Germar Knöchlein†

*Institut für Kernphysik, Johannes Gutenberg-Universität, D-55099 Mainz, Germany*

Cornelius Bennhold‡

*Center for Nuclear Studies, Department of Physics, The George Washington University,  
Washington, D.C., 20052*

### Abstract

We present a combined analysis of the new eta photoproduction data for total and differential cross sections, target asymmetry and photon asymmetry. Using basic assumptions, this allows a model-independent extraction of the  $E_{2-}$  and  $M_{2-}$  multipoles as well as resonance parameters of the  $D_{13}(1520)$  state. At higher energy, we show that the photon asymmetry is extremely sensitive to small multipoles that are excited by photons in the helicity 3/2 state. These could be, e.g., the  $F_{15}(1680)$ , the  $F_{17}(1990)$ , or the  $G_{17}(2190)$  resonances.

### INTRODUCTION

Over the last several years, eta photoproduction has demonstrated its potential as a new, powerful tool to selectively probe certain resonances that are difficult to explore with pions. It is well known that the low energy behavior of the eta production process is governed by the  $S_{11}(1535)$  resonance[1,2,3]. The recent, precise measurements of total and differential cross sections for eta photoproduction at low energies[4,5] have allowed determining the  $S_{11}(1535)$  resonance parameters with unprecedented precision. However, it is because of the overwhelming dominance of the  $S_{11}$  that the influence of other resonances in the same energy regime, such as the  $D_{13}(1520)$ , is difficult to discern. It has been pointed out[2] that polarization observables provide a new doorway to access these non-dominant resonances which relies on using the dominant  $E_{0+}$  multipole to interfere with a smaller multipole. Especially the polarized photon asymmetry was shown to be sensitive to the  $D_{13}(1520)$ . Recently, polarization data for the target and photon asymmetries in eta photoproduction were measured at ELSA[6] and GRAAL[7], respectively, for the first time. Taken together with the data for the unpolarized cross section from MAMI, they allow a determination of the  $D_{13}(1520)$  contribution in eta photoproduction.

### MULTIPOLE ANALYSIS

In the following all considerations refer to the c.m. frame. The three measured observables have the following representation in terms of the response functions defined in [8]:

$$\frac{d\sigma}{d\Omega} = \frac{|\vec{k}_\eta|}{|\vec{q}|} R_T^{00}, \quad (1)$$

$$T = \frac{R_T^{0y}}{R_T^{00}}, \quad (2)$$

$$\Sigma = -\frac{c R_{TT}^{00}}{R_T^{00}}. \quad (3)$$

---

\*E-mail: tiator@kph.uni-mainz.de

†E-mail: knoechle@kph.uni-mainz.de

‡E-mail: bennhold@gwis2.circ.gwu.edu

Because of the overwhelming dominance of the  $S_{11}$  channel in eta photoproduction, the observables can be expressed in terms of  $s$ -wave multipoles and interferences of the  $s$  wave with other multipoles. In the CGLN basis this leads to an  $F_1$  dominance and the observables can simply be expressed as

$$R_T^{00} = |F_1|^2 - \text{Re} \left\{ 2 \cos \theta F_1^* F_2 - \sin^2 \theta F_1^* F_4 \right\}, \quad (4)$$

$$R_T^{0y} = 3 \sin \theta \text{Im} \{ F_1^* F_3 + \cos \theta F_1^* F_4 \}, \quad (5)$$

$${}^c R_{TT}^{00} = \text{Re} \{ F_1^* F_4 \}. \quad (6)$$

If we retain only interferences with  $p$ - and  $d$ -waves (an approximation that is valid at least up to 1 GeV photon lab energy) we obtain

$$\begin{aligned} R_T^{00} &= |E_{0+}|^2 - \text{Re} [E_{0+}^* (E_{2-} - 3M_{2-})] \\ &\quad + 2 \cos \theta \text{Re} [E_{0+}^* (3E_{1+} + M_{1+} - M_{1-})] \\ &\quad + 3 \cos^2 \theta \text{Re} [E_{0+}^* (E_{2-} - 3M_{2-})], \end{aligned} \quad (7)$$

$$\begin{aligned} R_T^{0y} &= 3 \sin \theta \text{Im} [E_{0+}^* (E_{1+} - M_{1+})] \\ &\quad - 3 \sin \theta \cos \theta \text{Im} [E_{0+}^* (E_{2-} + M_{2-})], \end{aligned} \quad (8)$$

$${}^c R_{TT}^{00} = -3 \sin^2 \theta \text{Re} [E_{0+}^* (E_{2-} + M_{2-})]. \quad (9)$$

With the following angle-independent quantities

$$a = |E_{0+}|^2 - \text{Re} [E_{0+}^* (E_{2-} - 3M_{2-})], \quad (10)$$

$$b = 2 \text{Re} [E_{0+}^* (3E_{1+} + M_{1+} - M_{1-})], \quad (11)$$

$$c = 3 \text{Re} [E_{0+}^* (E_{2-} - 3M_{2-})], \quad (12)$$

$$d = \frac{1}{a + \frac{1}{3}c} 3 \text{Im} [E_{0+}^* (E_{1+} - M_{1+})], \quad (13)$$

$$e = -3 \frac{1}{a + \frac{1}{3}c} \text{Im} [E_{0+}^* (E_{2-} + M_{2-})], \quad (14)$$

$$f = 3 \frac{1}{a + \frac{1}{3}c} \text{Re} [E_{0+}^* (E_{2-} + M_{2-})], \quad (15)$$

we can express the observables in a series of  $\cos \theta$  terms that can be fitted to the experimental data at various energies  $E_{\gamma,lab}$

$$\frac{d\sigma}{d\Omega} = \frac{|\vec{k}_\eta|}{|\vec{q}|} \left( a + b \cos \theta + c \cos^2 \theta \right), \quad (16)$$

$$T = \sin \theta (d + e \cos \theta), \quad (17)$$

$$\Sigma = f \sin^2 \theta. \quad (18)$$

It is remarkable that a combined analysis of the three above observables allows a determination of the  $d$ -wave contributions to eta photoproduction once the quantities  $a$ ,  $c$ ,  $e$  and  $f$  have been determined from experiment. Already with the knowledge of  $e$  and  $f$  the helicity  $3/2$  multipole  $B_{2-}$ , defined below, and the phase relative to the  $S_{11}$  channel can be determined:

$$|B_{2-}| \equiv |E_{2-} + M_{2-}| = \frac{\sqrt{e^2 + f^2}}{3\sqrt{a + c/3}}, \quad (19)$$

$$\tan(\phi_{E_{0+}} - \phi_{B_{2-}}) = \frac{e}{f}. \quad (20)$$

If one neglects electromagnetic effects from the background of eta photoproduction affecting the phase of the electric and magnetic multipoles differently ( $\phi_{E_{l\pm}} = \phi_{M_{l\pm}} = \phi_{l\pm}$ ), one can write

$$E_{l\pm} = |E_{l\pm}|e^{i\phi_{l\pm}}, \quad (21)$$

$$M_{l\pm} = |M_{l\pm}|e^{i\phi_{l\pm}}, \quad (22)$$

and one finds the following representation for the real and imaginary parts of the  $d$ -wave multipoles:

$$\text{Re}E_{2-} = \frac{1}{4}\sqrt{a + \frac{1}{3}c}(f \cos \phi_{0+} + e \sin \phi_{0+}) \left(1 + \frac{c}{3f}\right), \quad (23)$$

$$\text{Im}E_{2-} = \frac{1}{4}\sqrt{a + \frac{1}{3}c}(f \sin \phi_{0+} - e \cos \phi_{0+}) \left(1 + \frac{c}{3f}\right), \quad (24)$$

$$\text{Re}M_{2-} = \frac{1}{12}\sqrt{a + \frac{1}{3}c}(f \cos \phi_{0+} + e \sin \phi_{0+}) \left(1 - \frac{c}{f}\right), \quad (25)$$

$$\text{Im}M_{2-} = \frac{1}{12}\sqrt{a + \frac{1}{3}c}(f \sin \phi_{0+} - e \cos \phi_{0+}) \left(1 - \frac{c}{f}\right). \quad (26)$$

We note that this determination of the  $E_{2-}$  and  $M_{2-}$  multipoles is rather model independent. To be more explicit we list the assumptions used to arrive at the above formulae:

- Phase difference between electric and magnetic multipoles neglected,  $\phi_{E_{l\pm}} = \phi_{M_{l\pm}} = \phi_{l\pm}$
- Restriction to the truncated multipole representation of Eqs. (7), (8), (9)
- Knowledge of the phase of the  $E_{0+}$  multipole.

The last point deserves further discussion: From total cross section data [4] it is obvious that in the region of the  $S_{11}(1535)$  resonance the cross section can be perfectly fitted by a Breit–Wigner resonance resulting in  $s$ -wave dominated differential cross sections. An investigation of the background from the Born terms [2] yielded a very small eta–nucleon coupling constant. As a consequence, the  $E_{0+}$  multipole can be treated as being completely dominated by the  $S_{11}(1535)$  contribution, which, as shown in ref.[4], allows parametrizing it through a Breit–Wigner form. In principle, an arbitrary phase for the complex  $E_{0+}$  multipole could be added which is set equal to 0 by convention. For the complex  $E_{0+}$  multipole we use the Breit–Wigner parametrization

$$E_{0+} = -\sqrt{\frac{a}{4\pi}} \frac{\Gamma^* M^*}{M^{*2} - W^2 - iM^*\Gamma(W)}, \quad (27)$$

where  $W$  is the c.m. energy. The energy dependence of the resonance width is given by

$$\Gamma(W) = \Gamma^* \left( b_\eta \frac{|\vec{k}|}{|\vec{k}^*|} + b_\pi \frac{|\vec{k}_\pi|}{|\vec{k}_\pi^*|} + b_{\pi\pi} \right). \quad (28)$$

The analysis of the  $E_{0+}$  interference with the  $E_{2-}$  and  $M_{2-}$  multipoles determines the  $d$  wave multipoles and therefore the difference  $\phi_{2-} - \phi_{0+}$ . It does not yield direct information on  $\phi_{2-}$ . However, making the above assumptions for the  $E_{0+}$  multipole and thus the phase  $\phi_{0+}$  permits the determination of  $\phi_{2-}$ .

To perform a similar analysis of the  $p$ -wave multipoles more information from additional polarization observables is required; in particular, a measurement of the recoil polarization would be very helpful. As before we obtain

$$P = \frac{R_T^{y0}}{R_T^{00}}, \quad (29)$$

$$= \sin \theta (g + h \cos \theta) \quad (30)$$

$$(31)$$

with

$$g = -\frac{1}{a + \frac{1}{3}c} \text{Im} [E_{0+}^* (2M_{1-} + 3E_{1+} + M_{1+})], \quad (32)$$

$$h = 3\frac{1}{a + \frac{1}{3}c} \text{Im} [E_{0+}^* (E_{2-} - 3M_{2-})]. \quad (33)$$

After performing single-energy fits we used a polynomial fit to the energy dependence of the coefficients  $a$ ,  $b$ ,  $c$ ,  $d$ ,  $e$  and  $f$  in order to arrive at a global (energy dependent) solution for the multipoles. This has several advantages: First the experimental data have been obtained in different set-ups at different labs, thus their energy bins do not match each other. Second, except for quantity  $a$  that is in principle determined already by the total cross section, all other quantities contain considerable error bars, therefore, a combined fit can reduce the uncertainty of individual measurements considerably. In a simple Taylor expansion in terms of the eta momentum with only 1-3 parameters in each coefficient we obtain good results for an energy region from threshold up to about 900 MeV.

## RESULTS

Fig. 1 shows 4 out of 10 angular distributions measured by the TAPS collaboration at Mainz [4] in the energy range between 716 and 790 MeV. While our isobar model falls a bit low close to threshold, a perfect fit is possible using the Ansatz in Eq. (16). Our results for the coefficients  $a$ ,  $b$  and  $c$  agree perfectly with the results obtained in Ref. [4]. As mentioned before, the  $a$  coefficient can be fitted to a Breit-Wigner form with an energy-dependent width leading, e.g., to parameters of  $M^* = (1549 \pm 8) \text{MeV}$ ,  $\Gamma_R = (202 \pm 35) \text{MeV}$  and an absolute value of the  $s$ -wave multipole at threshold,  $|E_{0+}| = 16.14 \cdot 10^{-3} / m_\pi^+$  (Fit 1, Ref. [4]). For our purpose here it is more convenient to use a general polynomial expansion as mentioned above.

Fig. 2 shows the target polarization with the preliminary data from Bonn[6]. Here our isobar model fails to reproduce the angular shape of the data. In particular there is no node in our calculation and the role of the  $D_{13}$  resonance plays a very small and insignificant role. In our previous coupled channel analysis the  $D_{13}$  resonance came out much stronger and a node developed, however, with a minus sign at forward and a positive sign at backward angles. This is opposite to the experimental observation and, as we will see later, indicates a drastically different relative phase between  $s$ - and  $d$ -waves. With the ansatz of Eq. (17) we can fit the data and obtain a node at low energies that disappears around 800 MeV.

In Fig. 3 we show our isobar calculations for the photon asymmetry. This observable has been measured recently at GRAAL [7], however, the data are still in the analysis. A preliminary comparison, however, shows general agreement for energies below 1 GeV. From our

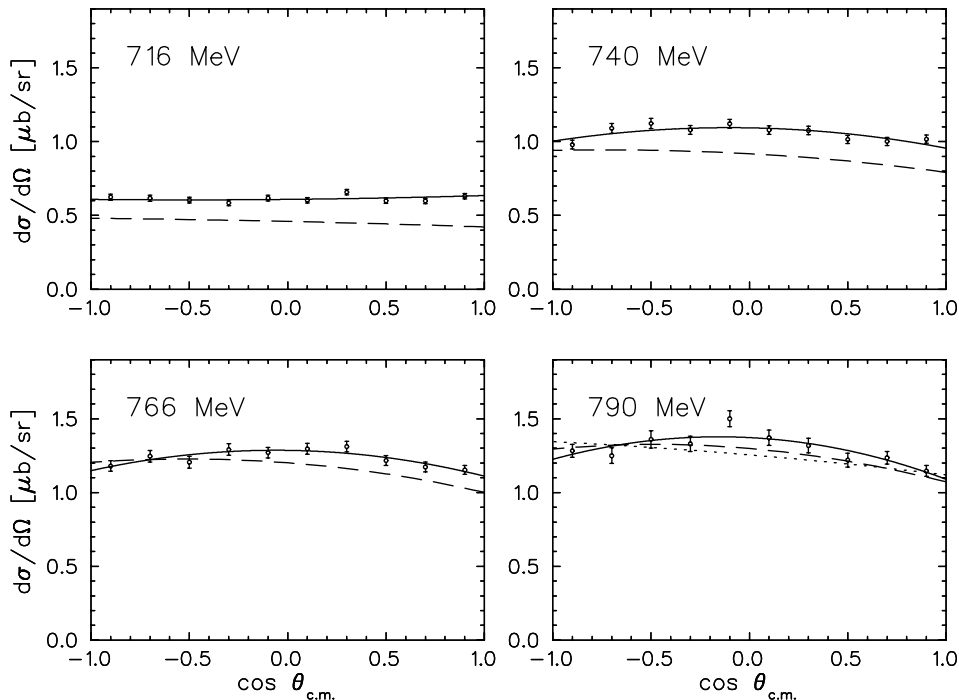
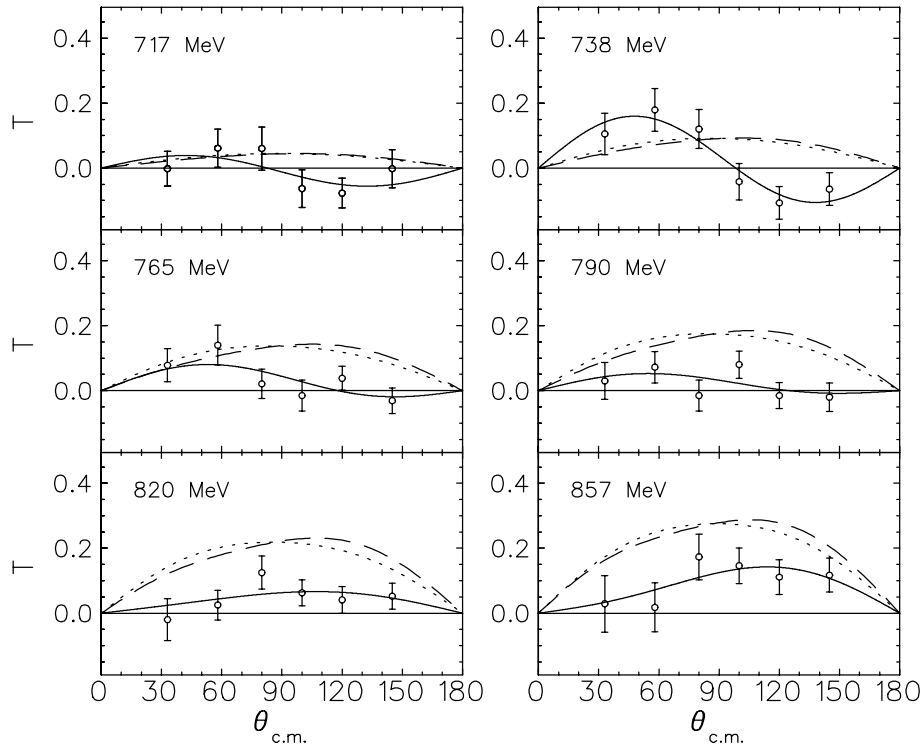


**Figure 1.** Differential cross section for  $p(\gamma,\eta)p$ . The solid lines show the fit to the experimental data of Krusche et al. [4]. The dashed lines show our calculations in the isobar model [8]. The dotted line at the highest photon lab energy of  $790\text{MeV}$  are obtained from our calculations when the  $D_{13}$  resonance is turned off.

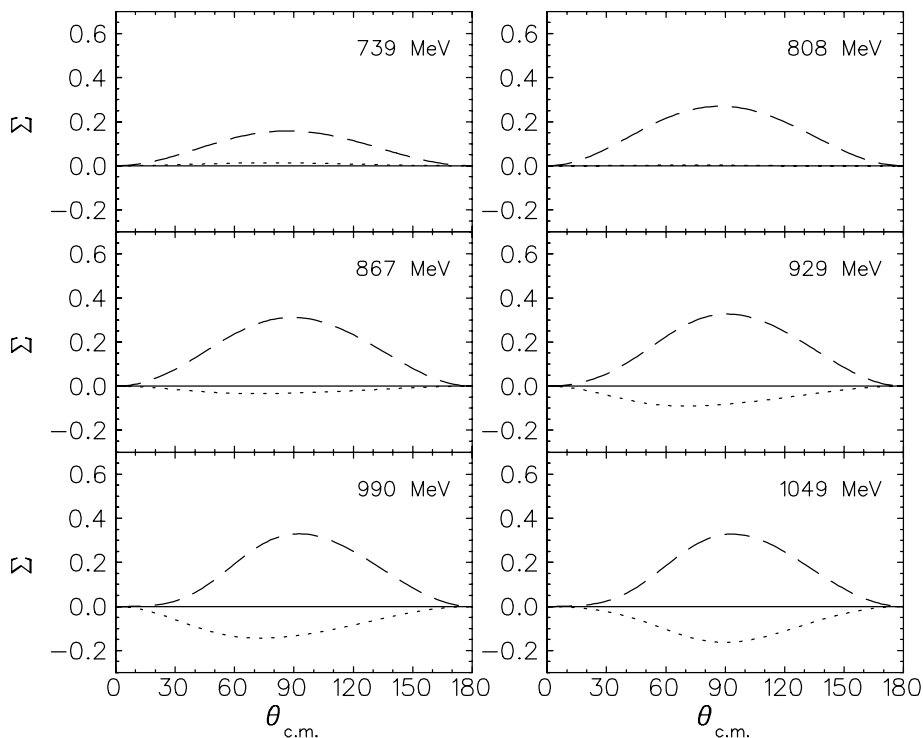
calculations the importance of the  $D_{13}$  channel for the photon asymmetry becomes obvious. Without this nucleon resonance, the asymmetry would be almost zero up to about 900 MeV. Even as the experimental data for the photon asymmetry are not yet available we can already perform a preliminary analysis of the  $D_{13}$  multipoles under the constraint of the photon asymmetries determined by our isobar model. In this case, all coefficients of Eqs. (10-15) are available and we can evaluate the  $d$ -wave multipoles using Eqs. (21-24). As mentioned before, the solution for the individual multipoles  $E_{2-}$  and  $M_{2-}$  requires the additional assumption for the phase of the  $s$ -wave amplitude. This is taken from the Breit-Wigner Ansatz Eqs. (27-28) with the parameters of fit 1 in Ref. [4]. Of course, this form is rather ad hoc, however, comparing with coupled channels calculations [9,10] we find that the results of these very different approaches agree very well not only for the absolute magnitude of the  $s$ -wave but also for the phase.

Fig. 4 shows the result of our multipole analysis and compares it with our isobar model calculation. The biggest difference occurs in the relative phase between the  $s$ - and  $d$ -waves. As shown in Eq. (20) this phase difference is model independent. If we consider two Breit-Wigner type resonances for both,  $S_{11}(1535)$  and  $D_{13}(1520)$  this phase difference would be rather constant as both resonances are very close in their energy position and, furthermore, have a similar resonance width. From the fact that the  $S_{11}$  is a bit higher in energy, the phase difference  $\Phi_0 - \Phi_2$  should be negative as is shown in the figure as the dotted line.

From the above analysis we conclude that this completely unexpected discrepancy is directly connected to the node structure of the target asymmetry. Without a node or with a node but an  $e$ -coefficient of opposite sign, the phase difference would be much smaller and



**Figure 2.** Target asymmetry for  $p(\gamma, \eta)p$ . The dashed and dotted lines show our calculations in the isobar model [8] with and without the  $D_{13}(1520)$  resonance. The solid line is the result of our fit to the experimental data of [6].



**Figure 3.** Photon asymmetry for  $p(\gamma, \eta)p$ . The dashed and dotted lines show our calculations in the isobar model [8] with and without the  $D_{13}(1520)$  resonance.

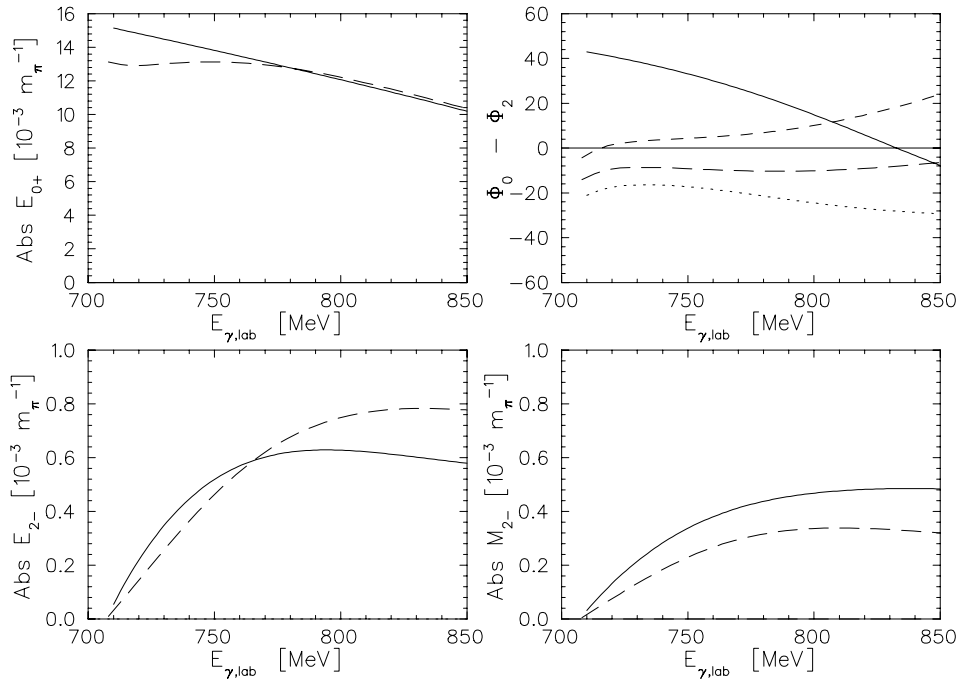


**Figure 4.** Result of the multipole analysis for  $s$ - and  $d$ - waves. The solid lines show the result of the fit. The short and long dashed lines are obtained from the isobar model. In the upper right figure we compare the phase difference of our fit with the isobar model. The short and long dashed curves show the difference obtained with the  $E_{2-}$  and  $M_{2-}$ , respectively. The dotted line is the difference of two Breit-Wigner forms.

closer to our model calculations.

## ETA PHOTOPRODUCTION AT HIGHER ENERGIES

The most remarkable fact of eta photoproduction in the low energy region is the strong dominance of the  $S_{11}$  channel. Whether it occurs from a  $N^*$  resonance, which is the most likely case, or from different mechanism is a very interesting question and subject of many ongoing investigations. In the experiment it shows up as a flat angular distribution and only very precise data can observe some tiny angular modulation as found by the Mainz experiment [4]. At Bonn, angular distributions of the differential cross section have been measured up to 1.15 GeV [11] with no evidence for a break-down of the  $s$ -wave dominance. Therefore, we can speculate that this dominance continues up to even higher energies. Theoretically, this could be understood in terms of very small branching ratios for nucleon resonances into the  $\eta N$  channel. For all resonances except the  $S_{11}(1535)$  the branching ratio is below 1%, or in most cases even below 0.1%. In the case of the  $D_{13}(1520)$  resonance this ratio is also assumed around 0.1%, however, an average number is no longer quoted in the Particle Data Tables [12]. Only branching ratios for the two  $S_{11}$  resonances remain. As we have shown in the last Section, the photon asymmetry is a very sensitive probe for even tiny branching ratios such as the  $D_{13}$  resonance.

In the following, we demonstrate that this is especially the case for nucleon resonances with strong helicity 3/2 couplings  $A_{3/2}$ . In Table 1 we list all entries for  $N^*$  resonances with isospin 1/2. From this table one finds the  $D_{13}$  as the strongest candidate to show up in the photon asymmetry. However, other resonances include the  $F_{15}(1680)$  which plays an important role

in pion photoproduction and, furthermore, the  $F_{17}(1990)$  and the  $G_{17}(2190)$  that are less established in photoproduction reactions. Furthermore, since these numbers are determined from data in the pion photoproduction channel, surprises in the eta photoproduction channel are not only possible but indeed very likely.

Table 1. Photon couplings and multiplicities for  $N^*$  Resonances with helicity 3/2 excitation. The numbers are taken from PDG96[12], average numbers above and single quoted numbers (less certain) below the horizontal line.

$N^*$ Resonance	$A_{3/2}[10^{-3}GeV^{-1/2}]$	Multipoles
$D_{13}(1520)$	$+166 \pm 5$	$B_{2-} = E_{2-} + M_{2-}$
$D_{15}(1675)$	$+15 \pm 9$	$B_{2+} = E_{2+} - M_{2+}$
$F_{15}(1680)$	$+133 \pm 12$	$B_{3-} = E_{3-} + M_{3-}$
$D_{13}(1700)$	$-2 \pm 24$	$B_{2-} = E_{2-} + M_{2-}$
$P_{13}(1720)$	$-19 \pm 20$	$B_{1+} = E_{1+} - M_{1+}$
$F_{17}(1990)$	$+86 \pm 60$	$B_{3+} = E_{3+} - M_{3+}$
$D_{13}(2080)$	$+17 \pm 11$	$B_{2-} = E_{2-} + M_{2-}$
$G_{17}(2190)$	$81 - 180$	$B_{4-} = E_{4-} + M_{4-}$

Assuming  $S$ -wave dominance and therefore  $F_1$ -dominance in the amplitude we can derive a general expression for the photon asymmetry,

$$\Sigma(\theta) = -\sin^2 \theta \operatorname{Re}[F_1^* F_4]/R_T^{00}, \quad (34)$$

$$= \sin^2 \theta \operatorname{Re}\left[E_{0+}^* \sum_{\ell \geq 2} (B_{\ell-} + B_{\ell+}) P_\ell''(\cos \theta)\right]/R_T^{00} \quad (35)$$

$$(36)$$

with  $B_{\ell-} = E_{\ell-} + M_{\ell-}$  and  $B_{\ell+} = E_{\ell+} - M_{\ell+}$ . Both multipole combinations are helicity 3/2 multipoles and for resonance excitation they are proportional to the photon couplings  $A_{3/2}$ . The helicity 1/2 couplings  $A_{1/2}$  do not enter here, they appear in the differential cross section and in the recoil polarization, e.g. as  $A_{2-} = (3M_{2-} - E_{2-})/2$ . Explicitly, we obtain up to  $\ell_{max} = 4$

$$\begin{aligned} \Sigma(\theta) = & \frac{\sin^2 \theta}{|E_{0+}|^2} \operatorname{Re}\left\{E_{0+}^* \left[3(B_{2-} + B_{2+}) - \frac{15}{2}(B_{4-} + B_{4+})\right.\right. \\ & \left.\left.+ 15(B_{3-} + B_{3+}) \cos \theta + \frac{105}{2}(B_{4-} + B_{4+}) \cos^2 \theta\right]\right\}. \end{aligned} \quad (37)$$

In Fig. 5 we demonstrate how such interferences of higher resonances with the  $S_{11}$  channel could show up in the photon asymmetry. Even if two small resonances of different multipolarity are excited in the same energy region they will produce a clear signal that will eventually allow determining  $\eta$  branching ratios down to values well below 0.1%.

## SUMMARY

We have demonstrated that polarization observables are a powerful tool in analyzing individual resonances in the eta photoproduction channel. The strong dominance of the  $S_{11}$  channel allows a much easier analysis compared to pion photoproduction. Furthermore, the

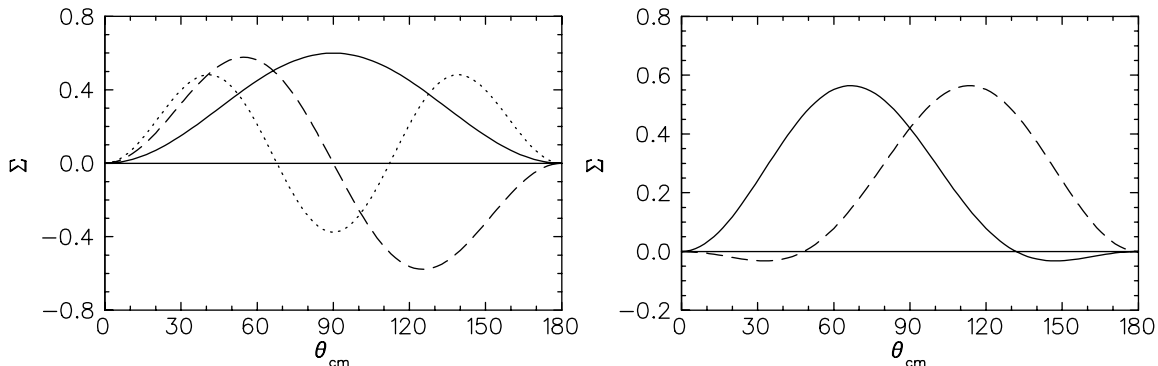


**Figure 5.** Possible signatures of  $N^*$  resonances in the photon asymmetry of eta photoproduction. The solid, dashed and dotted lines in the left figure show the angular distributions for the interference of the dominant  $S_{11}$  channel with an isolated  $D$ -,  $F$ , or  $G$ -wave, respectively. On the right, the situation of two resonances in the same energy region is demonstrated for a  $(D_{13}, F_{15})$  pair (solid curve) and a  $(D_{13}, F_{17})$  pair (dashed curve). Opposite signs are also possible if the photon or eta couplings of the resonances obtain a negative sign, see Table 1.

nonresonant background in eta physics appears to be small due to a very weak coupling of the eta to the nucleon. A combined analysis of differential cross section, photon asymmetry and target polarization allows a determination of  $s$ - and  $d$ -wave multipoles. The target polarization measured at Bonn reveals an unexpected phase shift between the  $S_{11}$  and  $D_{13}$  resonances that could lead to the conclusion that either of these resonances, perhaps the  $S_{11}$ , is heavily distorted or is even a completely different phenomenon, as frequently speculated. The new experiments therefore add another piece to the eta puzzle that makes the field of eta physics so exciting.

## REFERENCES

- [1] C. Bennhold and H. Tanabe, Nucl. Phys. **A530**, 625 (1991).
- [2] L. Tiator, C. Bennhold and S.S. Kamalov, Nucl. Phys. **A580**, 455 (1994).
- [3] M. Benmerrouche, N.C. Mukhopadhyay and J.-F. Zhang, Phys. Rev. **D51**, 3237 (1995).
- [4] B. Krusche et al., Phys Rev. Lett. **74**, 3736 (1995).
- [5] M. Wilhelm, Thesis (Bonn University, 1993).
- [6] A. Bock et al., submitted for publication in Phys. Rev. Lett. (1998).
- [7] J. Ajaka et al., contribution to this workshop.
- [8] G. Knöchlein, D. Drechsel and L. Tiator, Z. Phys. **A 352**, 327 (1995).
- [9] N. Kaiser, T. Waas and W. Weise, Nucl. Phys. **A 25** (1997) 297 and N. Kaiser, private communication.
- [10] T. Feuster and U. Mosel, nucl-th/9708051 and T. Feuster, private communication.
- [11] A. Bock, Thesis (Erlangen, 1997).
- [12] Review of Particle Physics, Particle Data Group, Phys. Rev. D **54** (1996) 1.